

Exploiting legacy dynamic simulators to accelerate steady state determination for chemical process plants

Kavouras, A¹, Kevrekidis, IG^{1,*}, Georgakis, C², Kelley, CT³

* corresponding author

Email: yannis@arnold.princeton.edu

¹ Department of Chemical Engineering, Princeton University, Princeton, NJ 08544, USA

² Department of Chemical and Biological Engineering, Tufts University, Science and Technology Center, Medford, MA 02155, USA

³ Department of Mathematics, Center for Research in Scientific Computation, North Carolina State University, Raleigh, NC 27695-8205, USA

Abstract: Given a legacy dynamic model of an open-loop unstable chemical process plant we construct a computational “wrapper” that extracts its steady states (both stable and unstable) and their dependence on input parameters. We apply this steady state determination approach to a challenge problem for process control presented by Downs and Vogel (1993), who also provided a FORTRAN process model. Using the FORTRAN model as a legacy dynamic simulator, we enable it to systematically compute steady states and their parametric dependence; our so-called “equation-free” approach is based on matrix-free iterative linear algebra methods. The existence of *inventories* and their interplay with the problem formulation and the solution procedure is clarified. Separation of time scales, when present, is taken advantage of in effectively reducing the model order and enhancing computational efficiency. This approach enables legacy dynamic simulators to calculate a multitude of linearized dynamic characteristics that could be used for controller design or optimization, for which they have not been intentionally designed.

Topical area: process systems engineering

Keywords: dynamic model, unstable processes, GMRES, inventory control, steady state

1 Introduction

Frequently in the chemical process industries simulators are developed that provide a dynamic representation of single units or integrated processes. Good dynamic simulators lead to a better understanding of the process, allow the exploration of case studies with varying design parameters, and provide insight towards linking manipulated vari-

ables with key process measurements. When a dynamic process model is sufficiently accurate, it can be used as a tool for optimization, or for controller design.

The source codes of such dynamic models are often not accessible, hence the term legacy code; even if they are, their size (and possibly lack of documentation) may be daunting when current users consider adapting them to new purposes. When alternative tasks such as optimization or controller design are considered, one may end up coding the model again from scratch for the new purpose, instead of reusing the available legacy dynamic simulator. Computational enabling technologies exist (see the discussion in Siettos et al. (2003)) that can fill this gap by wrapping a master code around the legacy dynamic simulator (the “time-stepper”, as we will refer to it through this paper). The master code uses the time-stepper as a computational experiment that provides output information for prescribed inputs; the master code prescribes initial conditions and parameter values and calls the time-stepper for a short time as a black box. The process states after the specified integration time are returned, and processed by the master code towards its ultimate task. The equations “hidden” in the black box code need not be known, nor are they ever extracted in closed form; important quantities (residuals, actions of Jacobians, derivatives with respect to parameters) are estimated from the time-stepper output on demand; for this reason we have termed the approach “equation-free”. In effect, we *solve* the equations coded in the black box dynamic simulator without ever obtaining them in closed form. It is worth noting that for our Tennessee-Eastman (TE) illustrative example the closed form equations *have* been extracted from the original source code (Ricker and Lee, 1995a) to be used for model predictive control purposes and dynamic optimization (Albuquerque et al., 1999).

A fundamental computational task in process modeling is the systematic determination of steady states. Computing the process steady states, as well as evaluating Jacobians and derivatives with respect to parameters at a steady state underpins both controller design and optimization computations. When a dynamic model is available, a simple, direct way to find *stable* steady states is to integrate in time until nothing changes; alternatively, when the steady state equations *are* available, fixed point algorithms like the Newton-Raphson method can be implemented using the Jacobian of the steady state equations and computational linear algebra. The steady states of the TE problem are, however, not so easy to find either way; the “reference” steady state given by Downs and Vogel (1993) is dynamically unstable, so that transient integration of the open-loop system moves away from it. Furthermore, the “legacy code” does not produce derivatives of the steady state equations as an output. Thus, performing Newton-Raphson to find steady states is not immediately implementable. Finally (and more importantly), because of the existence of two so-called *inventories* (see e.g. McAvoy and Ye (1994), Lyman and Georgakis (1995)) the steady state problem requires care in its definition. Inventories are commonly present in chemical process plants. Generally speaking an inventory is a vessel, in which the level does not affect the other steady state variables. Thus process models with inventories allow for infinitely many steady state solutions, parametrized by the levels of the inventories.

Problems of this nature are, mathematically, nonlinear eigenproblems: for some parameter values there are no solutions, and for other parameter values infinitely many solutions exist.

These complications have been tackled in different ways by many researchers over the last ten years, especially in low dimensional problems and in problems in which the equations are explicitly available rather than being hidden inside legacy codes. Feedback control techniques have been used to stabilize the open-loop unstable TE process and to obtain steady states. Time integration of the closed-loop dynamic system will then computationally locate the open-loop steady states; and by changing setpoints, the open as well as closed-loop steady state dependence on operating parameters can be tracked. Inventories, however, complicate the closed-loop controller design, and the associated zero eigenvalues also interfere with steady state approximation using Singular-Value-Decomposition and approximate inverses (Arkun and Downs, 1990; McAvoy, 1998).

In this paper we implement computational superstructures around the legacy code that enable the systematic computation of steady states (stable as well as unstable) and their dependence on parameters without the aid of feedback control. However, through augmentation with an appropriate number of so-called “pinning conditions”, well defined algebraic problems with isolated solutions can be formulated; we will discuss three different forms of such well posed augmented problems.

The TE legacy code can be called by our computational superstructure in two distinct formulations. In the first formulation the legacy code returns the *time derivatives* of the model variables at a prescribed state; we refer to this as the *right-hand-side formulation*. In the second formulation a call to the legacy code prescribes initial conditions for the state, performs *time integration* for a set *time horizon* starting from these initial conditions, and returns the system state at the end of this period; we call this the *time-stepper formulation*. Because of the legacy nature of the problem, which does not explicitly provide derivatives of the state equations, we use *matrix-free* numerical fixed point and continuation methods. Newton-GMRES is our method of choice here, and with the time-stepper based formulation of the steady state conditions, time integration of the legacy dynamic equations can lead to a significant reduction of the number of overall iterations; the existence of a separation of time scales in the TE problem combines with short time integration to what can be thought of as effective “on-line model reduction”. An early reference to the exploitation of GMRES for model reduction is given in Wigton et al. (1985).

The paper is organized as follows: In Section 2 we start with a brief presentation of the TE problem and some current approaches to the computation of its steady states. In Section 3 we discuss the interplay of inventories with fixed point computation and continuation and we derive three well posed augmentations of the steady state equations. We describe both the right-hand-side and the time-stepper steady state formulations. We recall a few basic features of Newton-GMRES and present our computational results. In Section 4 we make comparisons to other steady state computation approaches, and discuss the applicability of our implementation towards

control and optimization tasks, that require the computation of steady states as well as the local dynamic system characteristics.

2 The TE process and its time integration to steady state

A flowsheet that gives an overview of the units that constitute the TE process and illustrates the strong interlinking between them is given in Fig. 1. The model representation of the process (Downs and Vogel, 1993) consists of 50 state variables $\mathbf{x} \in \mathbf{R}^{50}$, 12 manipulated variables $\mathbf{u} \in \mathbf{R}^{12}$ and 41 measurements $\mathbf{y} \in \mathbf{R}^{41}$. The TE code returns the time derivatives $\mathbf{f}(\mathbf{x}, \mathbf{u})$ of the states - the right-hand-sides of the transient differential equations (1) at the current states \mathbf{x} and manipulated variables \mathbf{u} . In addition the measurements \mathbf{y} , which are dependent on the current \mathbf{x} alone, are returned by the call of the TE code.

$$\frac{d\mathbf{x}}{dt} = \mathbf{f}(\mathbf{x}, \mathbf{u}) \quad (1)$$

$$\mathbf{y} = \mathbf{g}(\mathbf{x}) \quad (2)$$

A random number generator that - if wanted - distorts the measurements with noise is also supplied with the routine; we did not use this feature. Base case values of a reference steady state \mathbf{x}_0 and \mathbf{u}_0 are also provided.

At the beginning of our study we linked the original Fortran TE code to Matlab as a mex file. We calculated the Jacobian $\partial\mathbf{f}/\partial\mathbf{x}$ at the reference steady state using numerical derivatives and obtained its eigenvalues through Matlab. As is well known, the eigenvalue analysis of the Jacobian at the base case values yields several very large negative eigenvalues, two zero-eigenvalues (computationally $\approx 10^{-6}$) and two pairs of complex conjugate eigenvalues with positive real parts. The large negative eigenvalues represent fast stable dynamics, while the positive real part eigenvalues indicate that the reference steady state is open-loop unstable. As a consequence, when time integration is performed to dynamically converge to the reference steady state, the process veers away from it and shuts down (violates operating constraints) within a short time. Fig. 2 shows the eigenvalues of the reference steady state Jacobian $\partial\mathbf{f}/\partial\mathbf{x}$. The eigenvalues with real parts larger than -10 (of which there are 19) are given in the upper part of the plot; the lower part of the plot shows all eigenvalues.

For stable systems it is common practice to determine steady states through time integration: when slightly perturbed from an isolated stable steady state, the simulation will asymptotically return to it. Depending on operating parameters, the TE process can also exhibit open-loop *stable* steady states and the transient open-loop response of the process after a perturbation from one such stable steady state (given in Tab. 1) is shown in Figs. 3, 4. The perturbation consisted in lowering the feed stream

of component A for a duration of 2.5 h process time (see Fig. 3). Temporary decrease or loss of the A feed stream was one scenario for disturbance rejection stipulated by Downs and Vogel (1993) and is considered one of the most challenging disturbances for control structures (Ricker and Lee, 1995b; Lyman and Georgakis, 1995; Price et al., 1994). For our representative open-loop stable steady state, the applied perturbation is spontaneously damped and the original steady state is asymptotically recovered after approximately 150 h process time. Time integration was here performed by a classical explicit Runge Kutta 4th order scheme with individual time steps 1.5 s.

At this representative stable steady state given in Tab. 1 two real part eigenvalues are again zero; but now the largest non-zero real part eigenvalue is -0.053, implying an overall *neutrally stable* system. An interesting feature of the dynamic simulation is, that the inventory levels of product separator and stripper do not regain their initial values after the other process measurements have equilibrated. It is well understood that this type of dynamic observation is characteristic of systems with inventories; the two inventories in the TE process are embodied in the two zero eigenvalues of the (singular) Jacobian. The second important feature is that these infinities do *not* occur at every operating parameter setting - for most operating parameter settings the open-loop problem *has no steady states*; as the operating parameters vary, these entire families of steady states appear only for special parameter combinations. At a given set of operating parameters, all state values remain constant when the holdup in the inventories varies; the nonzero eigenvalues of the Jacobian $\partial \mathbf{f} / \partial \mathbf{x}$ do, however, vary with the holdup, and the effect on the largest real part eigenvalue can be significant. For an increase of the levels of the product separator and the stripper at the TE process base case, the largest real part eigenvalue decreases, thus making the process less unstable. The reverse is observed when the levels of separator and stripper are decreased. The level of the product separator has a much stronger influence than that of the stripper - increasing the level of the product separator to 100 % while keeping the stripper level at 50 % decreases the leading eigenvalue real part to 2.528 whereas at the base case it is 3.065. These observations are easily rationalized, considering that the two vessels serve to dampen fluctuations of the concentrations of the liquid streams exiting from them. This effect of inventories on process dynamics can be taken advantage of in designing effective dynamic controllers for a process; for the nominal TE process in particular, dynamic operation is favorably affected by a large liquid holdup in the separator rather than the stripper.

In engineering practice, unstable steady states are stabilized through the addition of control loops. These give rise to closed-loop dynamic systems possessing *the same* steady states as the open-loop ones, but with different stability characteristics. Consider - as an illustration - the velocity formulation of a SISO PI controller with gain G , time constant τ and setpoint of a measurement y_{set} , which can be viewed as a transient differential equation: $u_{t+\Delta t} = u_t + G \cdot [(y_t - y_{t-\Delta t}) + (y_t - y_{set})/\tau \cdot \Delta t]$. In a control context one aims at transforming an open-loop *unstable* system like (1, 2) into a *stabilized* system through addition of an appropriate set of such feedback controllers. If the closed-loop system dynamics converge to the desired setpoint y_{set} ,

for an equilibrium value u_{set} of u_t , we have also found an open-loop steady state for $u = u_{set}$. This approach has been used for the numerical computation of TE model steady states (e.g. Subramanian and Georgakis (2004)), in the same way one would do it for physical experiments.

3 Steady state determination by continuation methods

In general, the solution of square systems of algebraic equations of the form $\mathbf{f}(\mathbf{x}, \mathbf{u}) = 0$ with $\mathbf{f} \in \mathbb{R}^n$ for the states $\mathbf{x} \in \mathbb{R}^n$ with prescribed parameters $\mathbf{u} \in \mathbb{R}^m$ is performed using continuation methods and contraction mappings like the Newton-Raphson algorithm. When the Jacobian is nonsingular, such algorithms trace both stable and unstable steady states families as the parameters (for our purposes, manipulated variables) \mathbf{u} are varied; there is no need for closing control loops to stabilize the system so that its steady states can be found by integration.

One iteratively solves the linear set of equations

$$\mathbf{f}(\mathbf{x}, \mathbf{u}) + \frac{\partial \mathbf{f}(\mathbf{x}, \mathbf{u})}{\partial \mathbf{x}} \cdot \delta \mathbf{x} = 0 \quad (3)$$

for $\delta \mathbf{x}$ and adding it to the current iterate \mathbf{x} until convergence. Inversion of the Jacobian $\partial \mathbf{f} / \partial \mathbf{x}$ through the standard Gauss algorithm requires, that the Jacobian has full rank i.e. is nonsingular.

We already know (from eigenvalue analysis, but also from physical reasoning about inventories) that the linearization of the TE equations is singular, and their steady states - if they exist - are not isolated. Since the Jacobian of the TE model is singular, standard Newton-Raphson fails; already McAvoy (1998) applied singular value decomposition to the Jacobian $\partial \mathbf{f} / \partial \mathbf{x}$, and reported the existence of two singular values equal to zero at the base case. Their analysis was carried out in the framework of Arkun and Downs (1990)'s method to identify gain matrices for processes that contain integrating tanks. McAvoy (1998) used a SVD based pseudo inverse to further converge the steady state of the base case given by Downs and Vogel (1993) (as the steady state they reported is not well converged) and then derive the gain matrix of the process through numerical derivatives.

While $\mathbf{f}(\mathbf{x}, \mathbf{u})$ is of dimension 50, $\partial \mathbf{f} / \partial \mathbf{x}$ is rank 48 (has two null vectors). In general, a change in one manipulated variable u_i results in a change $\partial \mathbf{f} / \partial u_i$ of \mathbf{f} , which is not in the range of the Jacobian matrix $\partial \mathbf{f} / \partial \mathbf{x}$. As we discussed, the full nonlinear problem has either no steady states or infinitely many. In order to obtain a well-defined problem, one augments the set of equations $\mathbf{f}(\mathbf{x}, \mathbf{u}) = 0$ from (1) with two additional algebraic equations (the so-called "pinning conditions"); more generally one would need as many pinning conditions as independent inventories in the problem. The pinning conditions select two out of the two-parameter infinity of steady state solutions. The augmented system has $n+2$ equations, and $n+2$ variables - the old n variables plus two more; typically the two additional unknowns will be two of the manipulated variables. In this approach the fact that not all 12 manipulated variables can be selected at will is clearly seen: 10 manipulated variables are prescribed, and the values of the remaining two for

which steady states exist result from the computation. Alternatively one can prescribe ten process measurements; the values of all twelve manipulated variables as well as a single steady state (out of the two-parameter infinity) will result from an appropriately augmented algebraic system. Once a single representative solution has been found, the entire two-parameter family can be routinely reconstructed using the null vectors of the steady state Jacobian. Clearly, while the inventories are vital for *dynamic* plant modeling, they are *effectively superfluous* for the determination of steady states. Note that in conventional PI control schemes each inventory is stabilized by manipulating one process variable in a closed-loop. An analogy therefore exists between well-posed fixed point/continuation problems (two additional pinning conditions, used to find two of the manipulated variables) and the closed-loop control approach (two control loops linking two manipulated variables with the two inventory holdups).

Augmented Steady State Problems

We want to find steady states of the problem (1), (2). In the right-hand-side formulation, we solve for the vector of time derivatives of the system state variables to be zero. In the time-stepper formulation, we solve for (4) to be zero, where $\Phi(\mathbf{x}_{t_0}, \mathbf{u}_{t_0}, \tau)$ is the result of integrating the system equations for a time horizon τ . Clearly, a steady state \mathbf{x} (a solution of (1) equal to zero $\mathbf{f}(\mathbf{x}, \mathbf{u}) = 0$) also satisfies (5) for all τ .

$$\mathbf{x}_{t_0+\tau} = \int_{t=t_0}^{t_0+\tau} \mathbf{f}(\mathbf{x}_{t_0}, \mathbf{u}_{t_0}) \cdot dt \equiv \Phi(\mathbf{x}_{t_0}, \mathbf{u}_{t_0}, \tau) \quad (4)$$

The time-stepper based equivalent to $\mathbf{f}(\mathbf{x}, \mathbf{u}) = 0$ for the determination of steady states based on the fixed point equation (4) is (5):

$$\hat{\mathbf{f}}(\mathbf{x}, \mathbf{u}, \tau) = \mathbf{x} - \Phi(\mathbf{x}, \mathbf{u}, \tau) = 0 \quad (5)$$

The following discussion applies therefore to both formulations.

As discussed, the TE process Jacobian (in both formulations!) has a rank deficiency of two, because of the two inventories. For parameter values for which steady states exist, they appear as a two-parameter infinity of solutions, parametrized by the inventory levels; the remaining steady state variables remain constant over the family. We have implemented three different ways of obtaining non-degenerate formulations of the steady state problem. We refer to the set of equations by \mathbf{F} and to their variables by \mathbf{X} .

Augmentation 1a: This formulation consists of the augmented set of equations

$$\mathbf{F}_{1a} = \begin{pmatrix} \mathbf{f}(\mathbf{x}, \mathbf{u}) \\ \mathbf{g}_l(\mathbf{x}) - \mathbf{y}_{l_{set}} \end{pmatrix} = 0 \quad (6)$$

where $\mathbf{f}(\mathbf{x}, \mathbf{u})$ is the vector of 50 time derivatives of state variables of the system and $\mathbf{g}_l(\mathbf{x})$ represents measurements affected by the inventory variables, which here

are the levels of the product separator and stripper bottoms. The two additional “pinning” constraints, which in this case are $y_{12} = g_{12}(\mathbf{x})$ and $y_{15} = g_{15}(\mathbf{x})$, select a single member of the two-parameter infinity of solutions; for the TE problem these correspond to “pinning” measurements 12 and 15 i.e. product separator and stripper levels. We solve for the steady state with 50 % level in the two inventories (product separator and stripper); we have 52 equations, and can therefore solve for 52 unknowns, which we can arrange in the column vector \mathbf{X}_{1a} .

$$\mathbf{X}_{1a} = \begin{pmatrix} \mathbf{x} \\ \mathbf{u}_d \end{pmatrix} \quad (7)$$

The column subvector \mathbf{u}_d is of dimension 2 and contains two *dependent* manipulated variables (the ones that we will choose to solve for after prescribing the remaining ten).

Our Newton step is then:

$$\begin{pmatrix} \mathbf{f}(\mathbf{x}, \mathbf{u}) \\ \mathbf{g}_l(\mathbf{x}) - \mathbf{y}_{l_{set}} \end{pmatrix} + \begin{bmatrix} \frac{\partial \mathbf{f}(\mathbf{x}, \mathbf{u})}{\partial \mathbf{x}} & \frac{\partial \mathbf{f}(\mathbf{x}, \mathbf{u})}{\partial \mathbf{u}_d} \\ \frac{\partial \mathbf{g}_l(\mathbf{x})}{\partial \mathbf{x}} & 0 \end{bmatrix} \cdot \begin{pmatrix} \delta \mathbf{x} \\ \delta \mathbf{u}_d \end{pmatrix} = 0 \quad (8)$$

The Newton converges when the augmented system above has a nonsingular Jacobian; our choice of two *dependent* manipulated variables is guided by this requirement. For this specific process any combination of two from the 12 manipulated variables of the TE problem would give a nonsingular Jacobian; certain choices, however, lead to better conditioned problems, or problems that do not easily hit saturation boundaries during parameter-space continuation. From the process side one might select as the new dependent variables two process flows that are closest in physical proximity and largest in effect on the two measurements, whose values are specified.

Augmentation 1b: A simple variation of the first formulation pins two *states*, involved in the equation(s) describing the rate of change of the inventory variables, instead of two measured variables. This formulation picks a solution out of the two parameter infinity by solving the set of equations

$$\mathbf{F}_{1b} = \begin{pmatrix} \mathbf{f}(\mathbf{x}, \mathbf{u}) \\ \mathbf{x}_l - \mathbf{x}_{l_{set}} \end{pmatrix} = 0 \quad (9)$$

where \mathbf{x}_l contains two elements of the complete state variable vector \mathbf{x} . These two variables \mathbf{x}_l must have non-zero contributions to the null-eigenvectors of $\partial \mathbf{f}(\mathbf{x}, \mathbf{u}) / \partial \mathbf{x}$, so that the two parameter infinity can be pinned down to a unique solution (again, any combination of two manipulated variables as the additional unknowns in the augmented system will lead to well-posed problems).

The associated Newton-Raphson scheme for augmentation 1b is:

$$\begin{pmatrix} \mathbf{f}(\mathbf{x}, \mathbf{u}) \\ \mathbf{x}_l - \mathbf{x}_{l_{set}} \end{pmatrix} + \begin{bmatrix} \frac{\partial \mathbf{f}(\mathbf{x}, \mathbf{u})}{\partial x_1} & \dots & \frac{\partial \mathbf{f}(\mathbf{x}, \mathbf{u})}{\partial x_{n-1}} & \frac{\partial \mathbf{f}(\mathbf{x}, \mathbf{u})}{\partial x_n} & \frac{\partial \mathbf{f}(\mathbf{x}, \mathbf{u})}{\partial \mathbf{u}_d} \\ 0 & \dots & 1 & \dots & 0 & 0 & 0 \\ 0 & \dots & \dots & 1 & \dots & 0 & 0 \end{bmatrix} \cdot \begin{pmatrix} \delta \mathbf{x} \\ \delta \mathbf{u}_d \end{pmatrix} = 0 \quad (10)$$

Augmentation 2: Here we substitute the last two lines of (9) i.e. the condition $\mathbf{x}_l = \mathbf{x}_{l_{set}}$ directly into $\mathbf{f}(\mathbf{x}, \mathbf{u}) = 0$, so that the equations for this augmentation are $\mathbf{F}_2 \equiv \mathbf{f}(\mathbf{x}, \mathbf{u}) = 0$. Instead of pinning at specified positions (like augmentations 1a and 1b) augmentation 2 removes two state variables, which represent inventories, as unknowns from the problem and replaces them (as unknowns) by an equal number of parameters (manipulated variables). The values of these manipulated variables will now be found as a function of the remaining parameters.

The vector of 50 unknowns now consists of the 48-long subvector \mathbf{x}_f , that contains all but two state variables, augmented by the two additional \mathbf{u}_d as above.

$$\mathbf{X}_2 = \begin{pmatrix} \mathbf{x}_f \\ \mathbf{u}_d \end{pmatrix} \quad (11)$$

This leads to the Newton-Raphson scheme:

$$\mathbf{f}(\mathbf{x}, \mathbf{u}) + \begin{bmatrix} \frac{\partial \mathbf{f}(\mathbf{x}, \mathbf{u})}{\partial \mathbf{x}_f} & \frac{\partial \mathbf{f}(\mathbf{x}, \mathbf{u})}{\partial \mathbf{u}_d} \end{bmatrix} \cdot \begin{pmatrix} \delta \mathbf{x}_f \\ \delta \mathbf{u}_d \end{pmatrix} = 0 \quad (12)$$

We refer to the sets of steady state equations of formulations 1a, 1b and 2, that use the time-stepper formulation $\hat{\mathbf{f}}(\mathbf{x}, \mathbf{u}, \Delta t)$ instead of the time derivatives $\mathbf{f}(\mathbf{x}, \mathbf{u})$ by $\hat{\mathbf{F}}$.

Clearly, the results of augmentation 2 will be the same as the results of augmentation 1b (they use the same pinning); augmentation 1a uses a different pinning, and so it will find *different representatives* of the family of solutions. Upon convergence, we obtain the values of the two dependent manipulated variables for which a two-parameter infinity of solutions exists, along with a single representative of the family (the one selected by our pinning). The rest of the steady state family for the manipulated variable values in question (the ten we prescribed and the two we found) is routinely obtained by using the null vectors of the degenerate problem Jacobian.

This discussion is independent of whether the code is available in a legacy form or explicitly (i.e., independently of whether we can evaluate the Jacobians from the equations, or we need to estimate them from the code). As a sanity check, we used the three above augmentations for the right-hand-side of the TE equations, using direct linear algebra (LU decomposition) on augmented Jacobians whose elements were estimated through finite differences from the TE code. We reproduced the optimal operating points given by Ricker (1995) (in “optimization modes” 1 and 4 of his paper).

We include here a representative one-parameter steady state branch (ten equidistant

steps) starting from the TE literature base case and ending on the stable steady state of Tab. 1 for which we presented transient simulations in Figs. 3 and 4. Figs. 5 and 6 show the variation, along this branch of the computed steady state measurements. The numbers on the abscissa correspond to the step along this branch; # 1 refers to the base case and # 11 is the stable steady state of Tab. 1.

At the stable steady state of Tab. 1 the process operating constraints stay well within the bounds for safe operation. As Ricker and Lee (1995b) described, a rise in the reactor temperature causes enhanced formation of byproduct F. This is apparently the case for the steady state of Tab. 1 as can be seen in a plot of the reactor feed concentration along the branch in Fig. 7. The product concentration at the stable steady state (not shown) undergoes only minor changes and the product stream of valuable components G+H even increases slightly when compared to the base case, while the production cost decreases slightly.

Using time-steppers to compute steady states

In principle steady states can be computed as fixed points of equations formulated with the time-stepper for *any* time reporting horizon τ . A number of papers in the recent numerical literature (see the work of Jarausch and Mackens (1987), Shroff and Keller (1993), Lust et al. (1998) as well as work in our group: Siettos et al. (2003), Kevrekidis et al. (2003, 2004), Kelley et al. (2004)) discuss the enabling of temporal simulation codes to converge on steady state solutions. For the TE problem, the fixed point equation $\mathbf{f}(\mathbf{x}, \mathbf{u}) = 0$ i.e. the steady state condition of (1) also gives rise to a rank-deficient Jacobian, and the augmentations discussed above will work equally well for the time-stepper formulation as they do for the right-hand-side formulation. The important element, however, in the time-stepper formulation, is the computation of the augmented Jacobian for Newton-Raphson. In principle, if equations are available, integration of variational and sensitivity equations (with codes like ODESSA, Leis and Kramer (1988)) will provide the derivatives with respect to initial conditions and parameter values that constitute Jacobian elements. The solution of the linear equations that constitute a Newton step, however, need not be carried out through direct linear algebra (LU decomposition); they can be carried out iteratively (through methods like GMRES: Saad (1981, 1984), Kelley (1995), Brown (1994)). Since GMRES computations actually require matrix-vector multiplications of the (Jacobian) matrix with a sequence of computed vectors, GMRES can be performed in a *matrix-free* fashion, using only calls to the integrator, as we will illustrate below. Partial derivative computations can thus be circumvented.

Our method of choice for the linear sets of equations that arise from Newton-Raphson augmented steady state problems (8), (10) and (12), both for the right-hand-side and for the time-stepper based formulations, was the iterative GMRES solver, which we now briefly review. GMRES is a subspace method for the iterative solution of sets of linear equations $\mathbf{A} \cdot \mathbf{x} + \mathbf{b} = 0$. Starting from the initial residual vector $\mathbf{r}_0 = \mathbf{A} \cdot \mathbf{x}_0 + \mathbf{b}$ a Krylov subspace (i.e. the span of a sequence of vectors arising from the matrix-vector products $\langle \mathbf{r}_0, \mathbf{A} \cdot \mathbf{r}_0, \mathbf{A}^2 \cdot \mathbf{r}_0, \mathbf{A}^3 \cdot \mathbf{r}_0, \dots \rangle$) is generated. When \mathbf{A} is the

Jacobian of a nonlinear function $\mathbf{f}(\mathbf{x}, \mathbf{u})$ the matrix vector products are retrieved from directional derivatives. Calculating a sequence of orthonormalized Krylov bases leads to the equality $\mathbf{A} \cdot \mathbf{Z}_k = \mathbf{Z}_{k+1} \cdot \mathbf{H}_{k+1}$, where \mathbf{Z}_k consists of the orthonormal basis vectors and \mathbf{H}_{k+1} is a Hessenberg matrix.

$$\mathbf{A} \cdot (\mathbf{x}_0 + \mathbf{Z}_k \cdot \mathbf{c}) + \mathbf{b} = \mathbf{Z}_{k+1} \cdot \mathbf{H}_{k+1} \cdot \mathbf{c} + \mathbf{r}_0 = \mathbf{r} \quad (13)$$

At the $k + 1$ step the linear least squares problem (14) of order $k + 1$ is solved to find the solution that minimizes the residual over the subspace.

$$\|\mathbf{H}_{k+1} \cdot \mathbf{c} + \|\mathbf{r}_0\| \cdot \mathbf{e}_1\| \rightarrow \min \quad (14)$$

An extensive survey of this family of Newton-Krylov methods can be found in Knoll and Keyes (2004). For our calculations with GMRES we used the code presented in Kelley (1995).

One Newton-Raphson step of (8), (10) and (12) is termed an ‘‘outer iteration’’ whereas the iterations to solve one set of linear equations are called ‘‘inner iterations’’. If the time-stepper (5) i.e. $\hat{\mathbf{f}}(\mathbf{x}, \mathbf{u}) = 0$ is used instead of $\mathbf{f}(\mathbf{x}, \mathbf{u}) = 0$, the iterative GMRES solver takes particular advantage of the eigenvalue structure of $\partial\Phi(\mathbf{x}, \mathbf{u}, \tau)/\partial\mathbf{x}$. Newton-GMRES solvers perform favourably with clustered eigenvalues of the Jacobian, which arises when using time-steppers to solve $\hat{\mathbf{f}}(\mathbf{x}, \mathbf{u}) = 0$; under such circumstances good solutions are often found after a relatively small number of iterations (in low-dimensional Krylov subspaces).

What makes this matrix-free computational approach an interesting one to combine with time-steppers, is that it can easily exploit time-scale separation when it is present in the problem of interest - and this is indeed the case in the TE process. Probably the first archival observation of this effect can be found in Wigton et al. (1985). It is obvious from the eigenvalue structure of the Jacobian $\partial\mathbf{f}/\partial\mathbf{x}$ given in Fig. 2 that the dynamics of the TE problem evolve on drastically different time scales. Integrating the differential equations with a time-stepper over large time horizons effectively reduces the problem size (in a linear problem it eliminates the components along eigenvectors associated with the fast stable dynamics from the output $\mathbf{x}_{t_0+\tau}$). Consider the eigenvalues of the Jacobian $\partial\Phi(\mathbf{x}, \mathbf{u}, \tau)/\partial\mathbf{x}$ (at steady state and for perfect integration these are $\exp(\lambda \cdot \tau)$, where τ is the reporting horizon and λ is the respective eigenvalues of the steady state Jacobian. As the reporting horizon of the time-stepper is increased, the fast eigenmodes of the time-stepper linearization move towards zero, while the slow (unstable) ones stay around (outside) the unit circle. For timestepping we used both a classical Runge Kutta explicit method of 4th order and an implicit Euler method. Due to the stiffness of the system we employed individual time steps of 1 s with the explicit method, while we covered the complete reporting horizon in *one single* time step with the implicit Euler method. When we evaluated the eigenvalues of $\partial\Phi(\mathbf{x}, \mathbf{u}, \tau)/\partial\mathbf{x}$ with the Runge Kutta time-stepper at the base case, the number of eigenvalues close to zero (absolute value below 10^{-4}) increased from 0 at reporting horizon 10 s to 8 at 50 s, 14 at 100 s, 18 at 500 s, 22 at 1000 s, 28 at 2000 s. Similar results were found

for time integration with the implicit Euler method. Fig. 8 shows the eigenvalues of the time-stepper evaluation for various reporting horizons at the base case operating point; once more, for perfect integration these ought to be $\exp(\lambda \cdot \tau)$, while for numerical integration they are approximations of $\exp(\lambda \cdot \tau)$ that depend on the particular method.

To highlight the advantages of the Newton-GMRES approach in the time-stepper formulation, we calculated a steady state of the TE process using all three augmentations 1a, 1b and 2. The steady state to be determined was designated by a change of the ratio of the D and E feed mass streams off the base case (decrease of u_1 by 0.25, increase of u_2 by 0.17391). For all three augmentations u_7 and u_8 were chosen as the *dependent* manipulated variables in \mathbf{u}_d . This corresponds to the typical inventory control scheme, where the underflows of the inventories are manipulated in order to control the vessel holdups. In augmentation 1b the two state variables x_{13} and x_{22} were arranged in \mathbf{x}_l to be pinned by the additional equations. In augmentation 2 these two state variables were kept at the values of the TE base case, such that \mathbf{x}_f contained all state variables but x_{13} and x_{22} . Convergence of the outer Newton-Raphson iteration was declared, when the quantity $\hat{\mathbf{F}}^T \cdot \hat{\mathbf{F}}$ fell below 10^{-10} .

The GMRES convergence is controlled by two tolerance parameters. The first (a so-called “forcing term”, η) is the ratio, by which the residual of the linear set of equations must be reduced before a sequence of inner GMRES iterations is declared successful, and the approximate solution of the linear set of equations (8), (10) or (12) is accepted. The second parameter limits the maximum number of inner iterations performed in one outer (Newton) iteration. An η of 0.1 performed satisfactorily for all computations reported here. We did not limit the maximum number of inner iterations to a smaller number than the problem size (i.e. we allowed for a full solution of the set of linear equations by the GMRES method if necessary; this never occurred in the time-stepper formulation). Restarted GMRES (see e.g. Kelley (1995)) is also an option for keeping the size of the system solved small; we did not use it in this paper.

Convergence results of the three augmentations for time-stepper based Newton-GMRES are given in Tabs. 2 and 3 for both a Runge Kutta and an implicit Euler time stepper. In particular Tab. 2 gives the total number of calls to time-stepper $\Phi(\mathbf{x}, \mathbf{u}, \Delta t)$ (for one reporting horizon) during all outer iterations until convergence. Note that each directional derivative, by which a direction is added to the Krylov subspace, involves one function call i.e. a call to the time-stepper over the reporting horizon. Furthermore, the number of outer Newton-Raphson iterations until convergence is displayed in Tab. 2. Integration over a time horizon requires repeated calls to the TE code. The total number of such calls of the TE code (right hand side evaluations of (1) incurred for a full steady state computation and the total CPU time for it is given in Tab. 3. Our Matlab programs and the TE code, that was connected to Matlab as a mex file, were run on Matlab Release 13 on a Pentium IV, 3 GHz computer under RedHat Linux.

The convergence results are strikingly different for the three problem augmentations. Augmentation 1a performed overall best with both time integration methods. Calling

the time-stepper over increasing reporting horizons reduces the required number of time-stepper calls significantly. The same tendency is observed with augmentation 1b, *but not with augmentation 2.*

Fig. 9 shows the full convergence history of augmentation 1a with the explicit Runge Kutta time-stepper and different reporting horizons. On the ordinate is the residual $\hat{\mathbf{F}}^T \cdot \hat{\mathbf{F}}$, on the abscissa is the cumulative number of time-stepper or function calls, which is equal to the cumulative number of inner GMRES iterations. Each marker in this plot represents the residual at an outer iteration, which was evaluated after completion of a sequence of inner GMRES iterations. Due to the inexact solution of the linear set of equations in the Newton-Raphson augmentation (8) by GMRES, the contraction of the residual with the Newton-Raphson iterations is slower than quadratic, even in the last few iterations. With increasing reporting horizon of the time-stepper, the decline of the residual versus the number of function calls becomes steeper. In fact, with augmentations 1a and 1b it takes about the same number of outer Newton-Raphson iterations to converge, but the dimension of the problem (the number of inner GMRES iterations for one approximate linear solve) reduces. The reason for this is that time integration, by eliminating the fast dynamic modes of the system, acts effectively as a *preconditioner*; the approximate linear solutions are obtained in an effectively smaller subspace than the original problem space. For augmentation 1a and the Runge Kutta time-stepper with a reporting horizon of 2000 s approximate linear solves can be obtained in, roughly, a 10-dimensional subspace (down from the original full space size of 52). As discussed in Kelley et al. (2004) the corresponding problem becomes a compact perturbation of the identity, the eigenvalues of its linearization cluster, and better performance is expected from GMRES.

For a stable process, of course, a call with a relatively long time horizon would require no iterations; yet it would take a large computational effort. We try to exploit separation of time scales, so that the effective preconditioning benefit from a relatively short integration - combined with the Newton-GMRES algorithm - outperforms both direct integration and Newton-GMRES on a right-hand-side formulation. Of course in many problems (e.g. split step dynamic simulators, or in cases where the inner time-stepper involves a stochastic or microscopic code, Kevrekidis et al. (2003), Kevrekidis et al. (2004)) the right-hand-side formulation is not an option. Due to the unstable nature of the TE process, the reporting horizon cannot be increased at will. Even if the input $\mathbf{x}_t, \mathbf{u}_t$ to the time-stepper is the steady state itself (to computer roundoff), it will veer away from the steady state if the open-loop unstable process is integrated over too long reporting horizons. A rule of thumb for the selection of an appropriate time horizon would put its inverse in the gap between the strong stable eigenvalues of the system linearization and the absolute values corresponding to the slow (both stable and unstable) eigendirections; so, fast components die (get slaved to slow ones), yet we do not integrate longer than necessary, and the unstable modes do not “explode” away from the steady state of interest.

Augmentation 1b shows the same qualitative behavior as in Fig. 9 with both time integration methods; in augmentation 2, however, an increase in the time reporting

horizon of the time-stepper does not reduce the number of function evaluations required for convergence (not shown). This suggests that the linearization of augmentation 2 does not exhibit eigenvalue clustering as 1a and 1b do. Plots of the eigenvalues of the Jacobian $d\hat{\mathbf{F}}/d\mathbf{X}$ of augmentations 1a, 1b and 2 with the Runge Kutta time integration at the base case values are given in Figs. 10, 11 and 12. Augmentation 2 with the Runge Kutta time-stepper produces one negative real eigenvalue with large absolute value at reporting horizons 500 and 1000, not shown in Fig. 12. An important factor for the GMRES method to perform well on a linear set of equations is the clustering of the eigenvalues of the problem matrix (Kelley, 1995). We clearly see that the eigenvalues of augmentations 1a and 1b indeed form clusters as the reporting horizon of the time-stepper is increased and the GMRES-time-stepper approach effectively reduces the problem size. It appears that these advantageous clustering characteristics do not arise in augmentation 2, and we believe that this underlies the observation that the problem size does not effectively reduce with increasing time-reporting horizon.

It might be argued, that the convergence criterion used for comparison between the three formulations is not fair, because the norm $\hat{\mathbf{F}}^T \cdot \hat{\mathbf{F}}$ of the vector function scales differently with different problem augmentations and reporting horizons of the time-stepper. We thus also used - as a convergence criterion - the residual $\mathbf{f}^T \cdot \mathbf{f}$ of the right hand side of (1), which corresponds to the set of equations that shall ultimately be solved; this criterion is the same for all problem augmentations and reporting horizons. Yet, the trends presented above did not change.

In earlier work Kelley et al. (2004) used GMRES to perform pseudo-arclength continuation for steady states of dynamical systems using time-steppers. They found, that the augmentation of the system equations with one additional equation (the pseudo-arclength equation for continuation) does not destroy the eigenvalue clustering of the augmented system.

The crucial question for the viability of the legacy time-stepper based Newton-GMRES approach to steady state computation is, of course, under which circumstances it performs better than direct time integration. Clearly, if one needs to compute unstable branches of steady states or marginally stable solutions, integration is simply not an option. As we saw for the TE process, direct open-loop integration also does not constitute an option for problems with inventories, whether they be stable or unstable. If we do not know the right combination of manipulated variables, steady states simply do not exist. For problems with asymptotically stable steady states, performance depends drastically on the distribution of the eigenvalues of the Jacobian $\partial\mathbf{f}/\partial\mathbf{x}$ of the system differential equations (1). Time-stepper Newton-GMRES is in principle best suited for large systems, characterized by a few slow (possibly unstable) eigenmodes and a large majority of fast, stable eigenmodes.

One thing should be made clear at this point. Using several time steps of an implicit integrator, and performing the associated nonlinear solves, is clearly not an efficient way of solving a fixed point problem (a single nonlinear solve). The integrator is used here as a legacy code, a code that in principle one cannot modify. It is in this context that our approach can be useful, as well as in multiscale computation cases, where the

time evolution is performed by a code at a different level of description (e.g. kinetic Monte Carlo).

In our discussion of time-scale separation and the corresponding gap between the system eigenvalues, we assumed for simplicity that the short numerical integration was perfectly accurate; when numerical integrators are used, the eigenvalues of the linearized time-stepper are not any more exponentials of the system eigenvalues multiplied by the reporting horizon τ . What integration method is used will not change the fixed point, but may drastically change the eigenvalues of the timestepper linearization (large explicit steps may even render a stable steady state *numerically* unstable). These linearized numerical timestepper eigenvalues affect GMRES performance, as can be seen in Tab. 3. In our example we used both an explicit and an implicit time-stepper and found - for our computational protocols - different trends of the CPU time for steady state determination with GMRES, when the reporting horizon was increased. For the implicit Euler time-stepper, for example, we chose a single time-step equal to the entire reporting horizon. With reporting horizons larger than 100 s the time step size was unreasonable in terms of accuracy, yet the resulting dampening was beneficial for steady state determination. In fact the reduction of the CPU time and number of right hand side (1) evaluations for increasing reporting horizons with the implicit Euler and augmentations 1a and 1b (as shown in Tab. 3) is entirely due to the GMRES “effective model reduction” and the resulting reduction of required time-stepper calls. The savings in the GMRES matrix inversion due to a smaller number of basis directions is not significant here. In conclusion, an increasing reporting horizon increases the computational expense for time integration, while possibly leading to increased GMRES performance; optimal performance will result from balancing these two trends.

4 Further system augmentation

During continuation with chemical process models, operating limits of the process need to be observed and failure to do so results in process shutdown. In terms of the TE process, these shutdown limits are the pressure and temperature high limits in the reactor and the high or low limit of the reactor liquid level.

In the augmentations discussed above we used the minimum number of pinning conditions that would give a well-posed problem - we prescribed 10 manipulated variables and allowed two to be computed from the model. In principle we can now perform pseudo-arclength continuation along any one-parameter path in ten-dimensional manipulated variable space. To make sure, however, that we do not frequently encounter operating limits, we may want to explore this ten-dimensional space by adding further constraints that keep key system measurements at fixed levels away from operability boundaries. Additional such pinnings result in reduction of the number of independent manipulated variables (and corresponding growth of the number of dependent variables) - one additional dependent variable for each additional pinned measurement.

The constrained measurements \mathbf{y}_c given in (15) are augmented to augmentation 1a and thus the equations for constrained steady state determination (16) are derived.

$$\mathbf{g}_c(\mathbf{x}) - \mathbf{y}_c = 0 \quad (15)$$

$$\begin{pmatrix} \mathbf{f}(\mathbf{x}, \mathbf{u}) \\ \mathbf{g}_l(\mathbf{x}) - \mathbf{y}_{l_{set}} \\ \mathbf{g}_c(\mathbf{x}) - \mathbf{y}_c \end{pmatrix} = 0 \quad (16)$$

The associated Newton-Raphson scheme is (17), the variables are the states \mathbf{x} , the *dependent* manipulated variables \mathbf{u}_d and the manipulated variables \mathbf{u}_c .

$$\begin{pmatrix} \mathbf{f}(\mathbf{x}, \mathbf{u}) \\ \mathbf{g}_l(\mathbf{x}) - \mathbf{y}_{l_{set}} \\ \mathbf{g}_c(\mathbf{x}) - \mathbf{y}_c \end{pmatrix} + \begin{bmatrix} \frac{\partial \mathbf{f}(\mathbf{x}, \mathbf{u})}{\partial \mathbf{x}} & \frac{\partial \mathbf{f}(\mathbf{x}, \mathbf{u})}{\partial \mathbf{u}_d} & \frac{\partial \mathbf{f}(\mathbf{x}, \mathbf{u})}{\partial \mathbf{u}_c} \\ \frac{\partial \mathbf{g}_l(\mathbf{x})}{\partial \mathbf{x}} & 0 & 0 \\ \frac{\partial \mathbf{g}_c(\mathbf{x})}{\partial \mathbf{x}} & 0 & 0 \end{bmatrix} \cdot \begin{pmatrix} \delta \mathbf{x} \\ \delta \mathbf{u}_d \\ \delta \mathbf{u}_c \end{pmatrix} = 0 \quad (17)$$

In the same manner formulations 1b and 2 can be augmented to solve for constrained steady states.

Such additional augmentations find their counterpart in the closed-loop approach to steady state stabilization/computation - additional setpoints require further control loops and “slave” additional manipulated variables. Consider the set of control and output variables in control structure 2 in Lyman and Georgakis (1995): There, single SISO loops tie all manipulated variables (except for the agitator speed) to controlled variables in the process. The controlled variables are the reactor temperature, the recycle flow rate and the stripper underflow (measurements 9, 5, 17), the levels in the stripper, the separator and the reactor (measurements 8, 12, 15), and besides concentrations in the reactor feed, the purge and the product stream (measurements 23, 26, 27, 30, 38). Note that reactor pressure is not controlled by this control scheme.

In our steady state augmentation formulation, if we impose the same change of reactor temperature from 120.4 to 121.6 and select the same sets of additional prescribed measurements and dependent manipulated variables as Lyman and Georgakis (1995), the values of the manipulated variables we find are given in Tab. 4. Also given in Tab. 4 is an example, where the product flow rate is increased by 3.5 % with the remaining ten pinned measurements remaining at the base case TE process values.

Both cases of setpoint change show, that with the control structure proposed in Lyman and Georgakis (1995), the manipulated variable u_9 (stripper steam) undergoes extreme changes ensuing from the generic setpoint changes of reactor temperature and production rate; the control loop linking u_9 with the concentration of component E in the product stream may easily saturate. Ricker and Lee (1995a) also report that the stripper steam rate has negligible effect on the process behavior. Removing the stripper steam rate (manipulated variable u_9) and the concentration of component E in the

product stream (controlled variable y_{38}) from the set of control and output variables of the control structure yields a set of 62 equations with 2 independent manipulated variables. Keeping now u_9 at its base case value and continuing in reactor temperature - without attempting to pin y_{38} , which floats - we find that the reactor temperature can be increased to $y_9 = 128.2$ °C before one of the dependent manipulated variables hits its bound. In this particular case the compressor recycle valve position u_5 hits its lower bound. Continuation in the product flow rate shows that it can be increased by 13.1 % ($y_{17} = 25.95 m^3/h$) before the reactor pressure hits the high limit for normal operation of 2895 kPa.

Having an algorithm that easily computes and parametrically continues steady states subject to various sets of constraints (keeping a given set of measurements constant through varying a given set of manipulated variables) allows a systematic exploration of the system operability. In particular, one can explore whether generic setpoint changes can be in principle performed using prescribed sets of manipulated variables to keep all controlled measurements at their setpoints without control saturation. One can even envision pinning conditions that ask for a manipulated variable or state variable to *marginally attain saturation* as a computational approach for tracing operability boundaries.

5 Discussion and Conclusions

Steady states of a dynamic process simulator were determined through matrix-free techniques (Newton-GMRES) that employ sequences of input-output calls to the legacy code. Two formulations (a differential one, where the legacy code returns time-derivatives of the state variables, and an integral one, where it returns the result of integration over a time reporting horizon) can be used for this purpose. This computational approach does not require prior stabilization of unstable processes through closing control loops.

The adaptation of this approach to problems with inventories was explored. When working with dynamic models of chemical process plants, inventories give rise to certain computational problems. Inventories turn the steady state problem into a nonlinear eigenproblem with either zero or infinite families of solutions. Their steady state levels have no influence on the other process states such as streams, concentrations, pressures and temperatures nor on the inflow or outflow of the inventory itself. They are also associated with singular Jacobians (Arkun and Downs (1990)) and the steady state equations must be appropriately augmented to yield well-posed problems. The number of freely adjustable manipulated variables among the total of manipulated variables reduces by one for each inventory. For a steady state to exist, *dependent* manipulated variables need to be defined, whose values are determined by the solution procedure.

While using a time-stepper based Newton-GMRES to solve these appropriately augmented problems, we explored the effect of time scale separation and the time-stepper reporting horizon on GMRES performance. Increasing the time-stepper reporting horizon could lead under appropriate conditions to significant reduction of the GMRES

iterates (time-stepper calls) required for the linear solve at each Newton iteration. We presented results pertaining to the effects of different augmentations as well as different numerical integration methods for the time-stepper.

A systematic steady state computation/continuation routine can be a valuable tool for various purposes like stability analysis, controller design and optimization. Determination of steady state gains is valuable towards controller design; yet for problems with inventories and/or unstable setpoints these gains may be difficult to obtain (for the TE problem see (McAvoy and Ye, 1994)). Systematic constrained continuation (implemented through further augmentations, as just discussed) can provide useful diagnostics in strongly nonlinear problems for gain sign change and control saturation.

For optimization, where the steady state equations appear as constraints, a feasible approach can take advantage of a fast, systematic steady state solver to turn the problem into an unconstrained one of reduced dimension. If the steady state solver underlying a feasible optimization code is based on control loops and integration (Subramanian and Georgakis, 2004; McAvoy and Ye, 1994), the closed-loop stability requirement will limit the steady states one can find, and thus possibly affect the optimization. Note that, thanks to the open structure of the original TE Fortran source code, steady state optimization has been accomplished by linking the TE code to a standard optimization routine (Ricker, 1995).

It is interesting, especially for legacy numerical approaches (including time-stepper based ones) where derivatives are not available, to explore the applicability of more direct search techniques (such as Nelder-Mead or Hooke-Jeeves algorithms) which have been experiencing a revival in both literature and practice (Kolda et al., 2003). “Black box” steady state solvers, turning the problem into a feasible one, may be an asset in such computations. We can provide some supporting evidence for this statement: locating an open-loop stable steady state for the TE process (the one we presented in Tab. 1) was the result of a Nelder-Mead optimization, where our objective was to optimize steady state stability. In particular, we tried to minimize the largest real part of the eigenvalues of the TE linearization at steady state. We solved this as a feasible problem; our steady state solver underlying the objective function evaluation was a Newton-GMRES time-stepper based one, and the Nelder-Mead direct search algorithm was the one of Kelley (1999). The optimization was performed over four manipulated variables that were chosen as “design parameters” (numbers 5, 6, 10 and 11); the two dependent manipulated variables in our augmentation were 7 and 8, and the remaining ones were kept at the base case values. In a forthcoming paper we use this methodology for TE process optimization.

Acknowledgements: This work was supported by a research scholarship of the Max Kade foundation for Andreas Kavouras, which is gratefully acknowledged. I.G.K. also acknowledges the partial support of AFOSR (Dynamics and Control) and an NSF ITR grant.

Notation:

A	coefficient/mass matrix of a linear set of equations
b	coefficient vector of a linear set of equations
c	state vector \mathbf{x} projected on the Krylow subspace
f	function of the derivatives of the states towards time in the TE process
f	time-stepper based set of equations for steady state determination in the TE process
F	non-degenerate replacement for steady state equations f , formulations 1a, 1b and 2
g	correlation between state vector and measurements
H	Hessenberg matrix in GMRES method
t	time
r	residual vector of a linear set of equations
u	vector of manipulated variables
u_d	vector of <i>dependent</i> manipulated variables
x	state vector of the TE process, solution vector of a set of linear equations
x_f	reduced state vector of the TE process
X	variables of the non-degenerate steady state equations F = 0, formulations 1a, 1b and 2
y	measurements
Z_k	orthonormalized Krylow subspace with k basis vectors of the Jacobian in a Newton-GMRES solver

Greek letters:

λ	eigenvalue
Φ	right hand side of a time-stepper formulation of the differential evolution equation

References

- Downs, JJ, Vogel, EF. A plant wide industrial process control problem. *Comp. Chem. Eng.* 1993; 17 (3): 245 - 255
- Siettos, CI, Pantelides, CC, Kevrekidis, IG. Enabling Dynamic Process Simulators

- to Perform Alternative Tasks: A Time-Stepper-Based Toolkit for Computer-Aided Analysis. *Ind. Eng. Chem. Res.* 2003; 42 (26): 6795 - 6801
- Ricker, NL, Lee, JH. Nonlinear modeling and state estimation for the Tennessee Eastman challenge process. *Comp. Chem. Eng.* 1995a; 19 (9): 983 - 1005
- Albuquerque, J, Gopal, V, Staus, G, Biegler, LT, Ydstie, BE. Interior point SQP strategies for large-scale, structured process optimization problems. *Comp. Chem. Eng.* 1999; 23: 543 - 554
- McAvoy, TJ, Ye, N. Base control for the Tennessee Eastman problem. *Comp. Chem. Eng.* 1994; 18: 383 - 413
- Lyman, PR, Georgakis, C. Plant-Wide Control of the Tennessee Eastman Problem. *Comp. Chem. Eng.* 1995; 19 (3): 321 - 331
- Arkun, Y, Downs, J. A general method to calculate input-output gains and the relative gain array for integrating processes. *Comp. Chem. Eng.* 1990; 14(10): 1101 - 1110
- McAvoy, TJ. A methodology for screening level control structures in plantwide control systems. *Comp. Chem. Eng.* 1998; 22 (11): 1543 - 1552
- Wigton, LB, Yu, NJ, Young, DP. GMRES acceleration of computational fluid dynamics. *AIAA Conference 1985; A85 - 1494: 67 - 74*
- Ricker, NL, Lee JH. Nonlinear model predictive control of the Tennessee Eastman challenge process. *Comp. Chem. Eng.* 1995b; 19 (9): 961 - 981
- Price, RM, Lyman, PR, Georgakis, C. Throughput Manipulation in Plantwide Control Structures. *Ind. Eng. Chem. Res.* 1994; 33: 1197 - 1207
- Subramanian, S, Georgakis, C. A Methodology for the Steady-State Operability Analysis of Plantwide Systems. Submitted to *Ind. and Eng. Chem. Res.* in 2004
- Ricker, NL. Optimal steady-state operation of the Tennessee Eastman Challenge Process. *Comp. Chem. Eng.* 1995; 19 (9): 949 - 959
- Jarusch, H, Mackens, W. Solving Large Nonlinear Systems of Equations by an Adaptive Condensation Process. *Numer. Math.* 1987; 50: 633 - 653
- Shroff, GM, Keller, HB. Stabilization of unstable procedures: the recursive projection method. *SIAM J. Numer. Anal.* 1993; 30 (4): 1099 - 1120
- Lust, K, Roose, D, Spence, A, Champneys, AR. An adaptive Newton Picard algorithm with subspace iteration for computing periodic solutions. *SIAM J. Sci. Comp.* 1998; 19: 1188 - 1209
- Gear, CW, Hyman, JM, Kevrekidis, PG, Runborg, O, Theodoropoulos, K. Equation-free coarse-grained multiscale computation: enabling microscopic simulators to perform system-level tasks. *Comm. Math. Sciences* 2003; 1 (4): 715 - 762

- Kevrekidis, IG, Gear CW, Hummer, G. Equation-free: the computer-assisted analysis of complex, multiscale systems. *AIChE Journal* 2004; 50(7): 1346 - 1354
- Kelley, CT, Kevrekidis, YG, Qiao, L. Newton-Krylov solvers for time-steppers. Submitted to *SIAM Journal on Applied Dynamical Systems* 2004
- Leis, JR, Kramer, MA. The simultaneous solution and sensitivity analysis of systems described by ordinary differential equations. *ACM Transactions on Mathematical Software* 1988; 14 (1): 45 - 60
- Saad, Y. Krylov subspace methods for solving large unsymmetric linear systems. *Math. Comp.* 1981; 37: 105 - 126
- Saad, Y. Practical use of some Krylov subspace methods for solving indefinite and nonsymmetric linear systems. *SIAM J. of Sci. and Stat. Comp.* 1984; 5 (1): 203 - 228
- Kelley, CT. *Iterative Methods for Linear and Nonlinear Equations*. SIAM Series Frontiers in Applied Mathematics 1995, Volume 16
- Brown, PN, Hindmarsh, AC, Petzold, LR. Using Krylov methods in the solution of large-scale differential-algebraic systems. *SIAM J. Sci. Comput.* 1994; 15: 1467 - 1488
- Knoll, DA, Keyes, DE. Jacobian-free Newton-Krylov methods: a survey of approaches and applications. *Journal of Computational Physics* 2004; 193: 357 - 397
- Kolda, TG, Lewis, RM, Torczon, V. *Optimization by Direct Search: New perspectives on Some Classical and Modern Methods*. *SIAM Review* 2003; 45 (3): 385 - 482
- Kelley, CT. *Iterative Methods for Optimization*. SIAM Series Frontiers in Applied Mathematics 1999, Volume 19

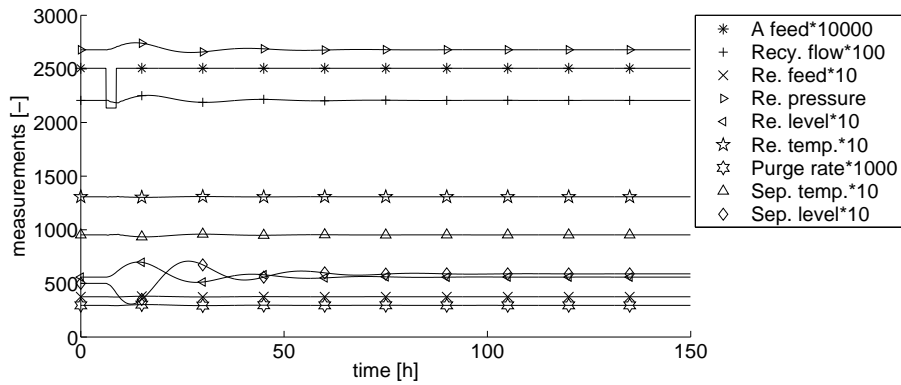


Figure 3: Process measurements 1 - stable steady state

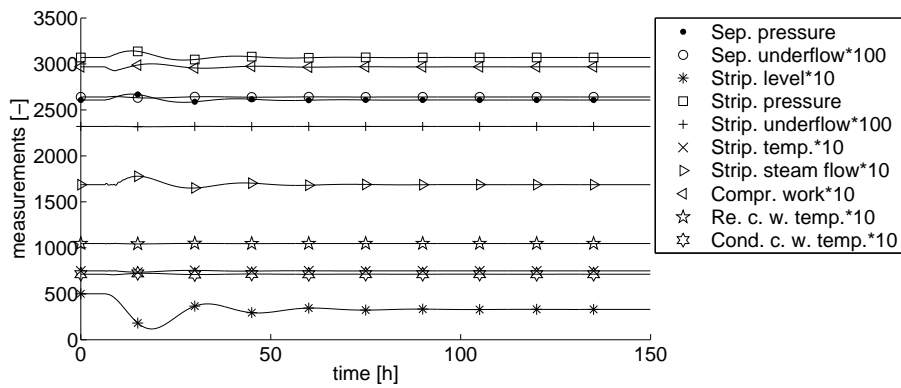


Figure 4: Picture measurements 2 - stable steady state

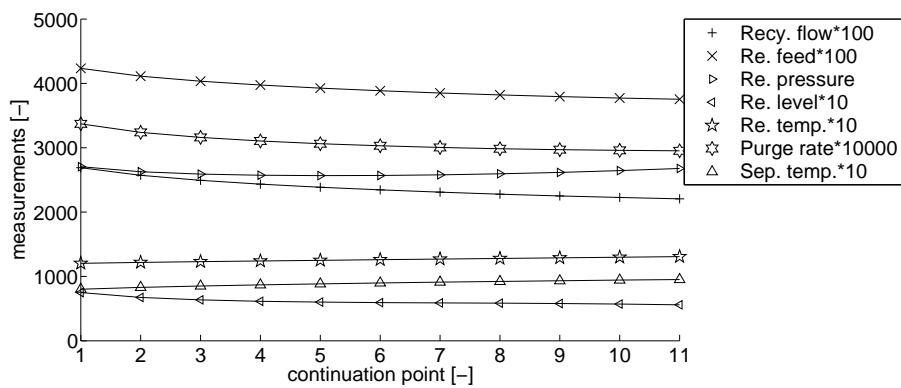


Figure 5: Continuation to stable steady state of Tab. 1 - measurements 1

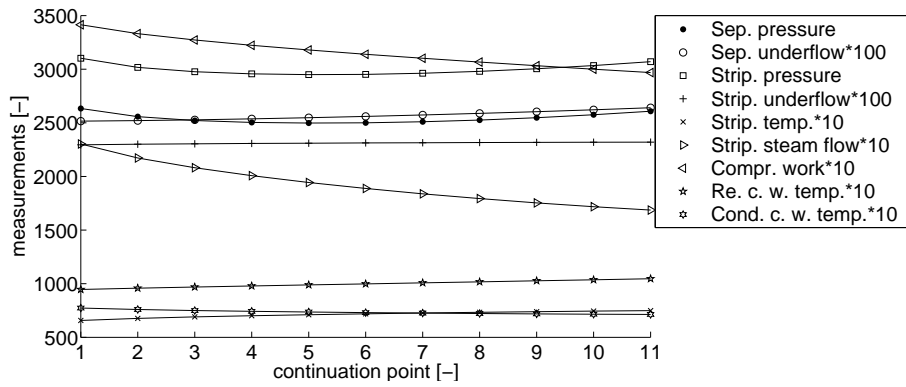


Figure 6: Continuation to stable steady state of Tab. 1 - measurements 2

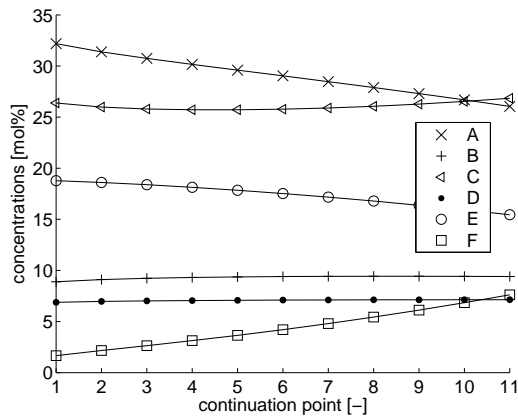


Figure 7: Continuation to stable steady state of Tab. 1 - reactor feed concentrations

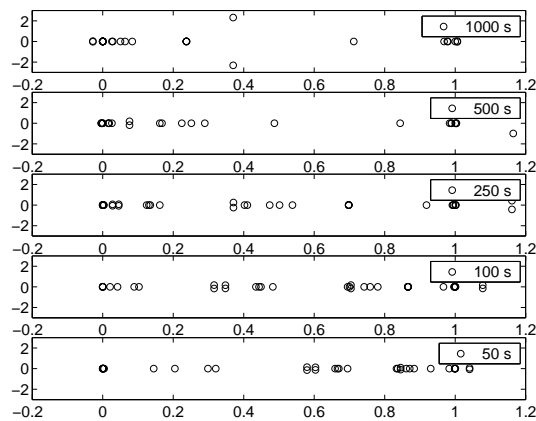


Figure 8: Plot of eigenvalues of the Jacobian $\partial\Phi/\partial\mathbf{x}$ of the Runge Kutta time-stepper at the base case

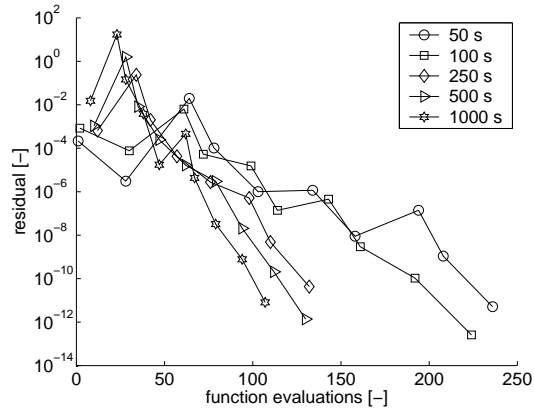


Figure 9: Convergence history of formulation 1a with the time-stepper

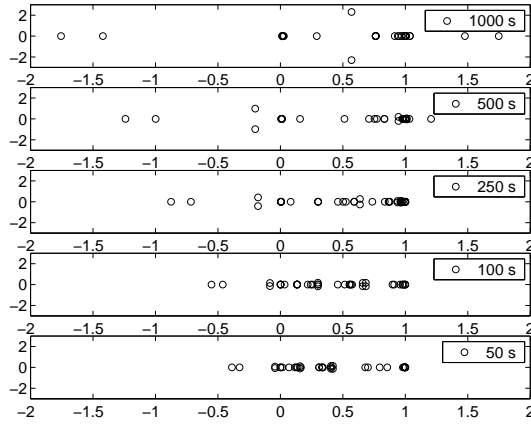


Figure 10: Plot of eigenvalues of Jacobian $d\hat{\mathbf{F}}_{1a}/d\mathbf{X}_{1a}$ at base case (formulation 1a with the Runge Kutta time stepper) at various reporting horizons Δt

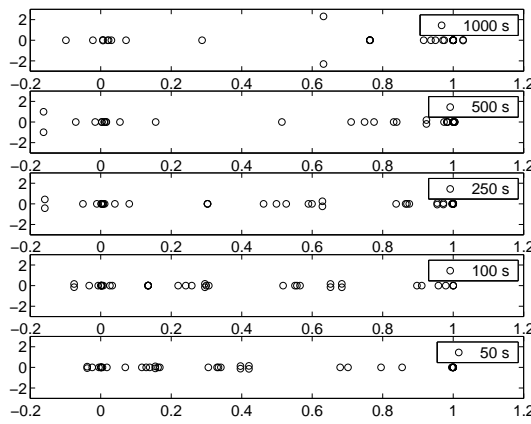


Figure 11: Plot of eigenvalues of Jacobian $d\hat{\mathbf{F}}_{1b}/d\mathbf{X}_{1b}$ at base case (formulation 1b with the Runge Kutta time stepper) at various reporting horizons Δt

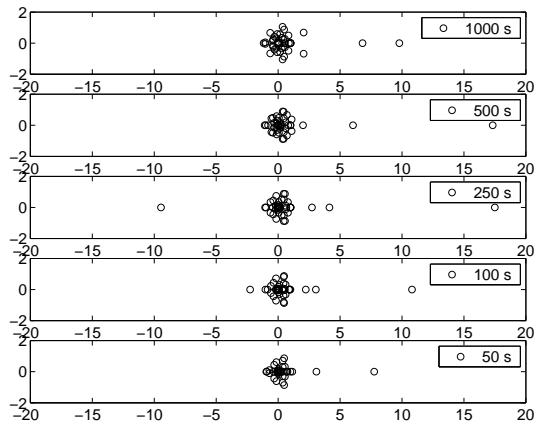


Figure 12: Plot of eigenvalues of Jacobian $d\hat{\mathbf{F}}_2/d\mathbf{X}_2$ at base case (formulation 2 with the Runge Kutta time-stepper) at various reporting horizons Δt

Tables:

Table 1: *Manipulated variables and key process measurements at an open-loop stable operating point of the TE process*

Manipulated variables [%]	
D feed flow u_1	63.053
E feed flow u_2	53.980
A feed flow u_3	24.644
A+C feed flow u_4	61.302
Compressor recycle u_5	22.881
Purge valve u_6	42.322
Separator underflow u_7	38.256
Product flow u_8	46.421
Stripper steam u_9	47.446
Reactor cooling water u_{10}	35.620
Condenser cooling water u_{11}	19.620
Agitator speed u_{12}	50.000
Measurements	
Reactor pressure y_7 [mbar]	2678
Reactor level y_8 [%]	55.9
Reactor temperature y_9 [°C]	130.7
Stripper underflow y_{17} [m^3/h]	23.2

Table 2: Number of time-stepper calls and number of Newton-Raphson iterations for the continuation step with formulations 1a, 1b and 2 as a function of the reporting horizon Δt

Δt	1a	1b	2	1a	1b	2
Runge Kutta	TS calls			NR iters.		
10 s	201	315	406	8	14	11
50 s	236	252	408	10	10	10
100 s	224	208	367	10	9	9
250 s	132	185	365	8	10	9
500 s	130	164	361	9	11	9
1000 s	107	96	384	10	8	12
2000 s	96	102	399	12	14	13
3000 s	96	99	416	12	12	15
Implicit Euler						
50 s	245	251	321	10	10	8
100 s	226	247	407	11	10	10
500 s	111	164	374	9	11	10
1000 s	98	113	338	9	8	10
5000 s	62	85		7	8	

Table 3: Total number of calls of the right hand side of (1) and CPU time for the continuation step with formulations 1a, 1b and 2 as a function of the reporting horizon Δt

Δt	1a	1b	2	1a	1b	2
Runge Kutta	$10^3 \times$ RHS calls			CPU time		
10 s	8.7	13.7	17.1	0.6	1.0	1.2
50 s	51.2	54.4	85.6	2.4	2.6	4.0
100 s	97.6	90.4	154	4.3	4.0	6.7
250 s	148	205	383	6.2	8.7	16.0
500 s	296	372	758	12.3	15.4	31.3
1000 s	508	448	1632	20.9	18.5	67.1
2000 s	960	1040	3400	39.3	42.5	139.6
3000 s	1440	1476	5352	58.9	60.8	218.1
Implicit Euler						
50 s	44.5	44.7	61.8	3.4	3.4	4.8
100 s	42.0	49.4	77.5	3.2	3.9	6.0
500 s	23.8	34.2	84.8	1.9	2.7	6.8
1000 s	22.5	24.2	75.6	1.8	1.9	6.8
5000 s	14.8	19.3		1.2	1.6	

Table 4: Manipulated variables of the TE process at base case, at reactor temperature $y_9 = 121.6$ °C and at a product flow rate that is increased by 3.5 % ($y_{17} = 23.752m^3/h$) with the set of control and output variables used in control structure 2 in Lyman and Georgakis (1995)

MV	base case	$y_9 = 121.6$ °C	$y_{17} = 23.752m^3/h$
1	63.0526	63.6584	64.1466
2	53.9797	54.2347	56.1574
3	24.6436	25.5426	25.0296
4	61.3019	61.6400	63.0798
5	22.2100	18.9699	22.7734
6	40.0637	41.6996	40.2187
7	38.1003	37.6623	39.8558
8	46.5342	46.8157	47.8766
9	47.4457	4.4434	95.6305
10	41.1058	40.8412	42.4343
11	18.1135	16.1119	20.8812